Performance Evaluation of Interference and Cell Loading in UMTS Networks

Kenji Leibnitz and Armin Krauß

Institute of Computer Science, University of Würzburg, Am Hubland, D-97074 Würzburg, Germany

The introduction of third generation (3G) wireless systems operating with Wideband Code Division Multiple Access (WCDMA) will offer new data services with bit rates of up to 2 Mbps and varying quality of service requirements in terms of received bit-energy-to-noise ratio. In order to reduce the interference in the cell and thus maximize the capacity WCDMA systems require a tight power control mechanism. In this paper we will present a performance evaluation of the WCDMA uplink power control loops by means of simulation. Our main goal is to investigate the influence of the traffic, given by the spatial user distribution and their data services, on the interference in a cell. We will also show that it is possible to use approximations of the power control loops to evaluate more complex scenarios.

1. INTRODUCTION

Wideband Code Division Multiple Access (WCDMA) technology will be the most prominent access technology over the air interface for the upcoming third generation wireless systems (3G) [1]. Contrary to second generation networks which are rather limited to voice services, 3G systems like the *Universal Mobile Telecommunication System* (UMTS) in Europe are dedicated to offer data services with high bit rates and flexible capabilities. Another important difference is that due to WCDMA the cell capacity is no longer a fixed term, but will be limited on the *uplink* (mobile-to-base station path) by the interference created by the users and on the *downlink* (base station-to-mobile path) by the maximum transmission power of the base station [2]. Thus, the uplink capacity depends on the spatial distribution of the users [3] and their individual services given by the data rate and the activity factor.

This interference limitation leads to the necessity of reducing the transmission power of each user to a minimum. Mobile stations (MS) will be located at varying distances from the base station (NodeB). However, if a mobile near the NodeB transmits with a power level that is too high, it causes too much interference for other MS farther away ("near-far" problem). Additionally, due to shadowing and multi-path fading there will be variations in the signal strength received at the NodeB. All of this is overcome by power control loops performed on the uplink. With this power control mechanism the NodeB tries to perform a balancing of the received *bit-energy-to-noise ratio* (E_b/N_0) of all users in the cell. For these reasons, an evaluation of the capacity depends heavily on the performance of the power control loops.

Models of closed loop power control algorithms have been studied by many authors in the past. While some of the studies contain analytical approaches, e.g. [4–8], many researchers have also used simulations to investigate the effects of the system parameters on the efficiency

of power control, e.g. see [9–13]. Most of these previously mentioned studies focus on IS-95 systems operating with a single class of users, however, the complexity of the model increases rapidly when considering several different classes of users. This often leads to the case where an analytical performance evaluation reaches its limits and evaluation by simulation is required [14–16].

In this paper we will describe a simulation model of the uplink closed loop power control in UMTS. This model will permit an evaluation of the influence of the user distribution and the traffic mix on the interference in a cell. The user distribution will be modeled with a homogeneous spatial Poisson process and we will derive empirical distributions of the interference caused by the users in the same cell and users from neighboring cells. Based on the total interference, we will show how the traffic density impacts the cell loading factor.

This paper is organized as follows. In Section 2 we will give a detailed description of the closed loop power control model and describe an approximation model that reduces the computation time. We will show the relationship between the user density, traffic mix, and the interference in Section 3 and demonstrate that the cell loading factor is a useful indicator for cell capacity. Numerical results will be given in Section 4 that show the applicability of the approximation method which permits an evaluation of complex real world scenarios.

2. MODELING OF UMTS POWER CONTROL
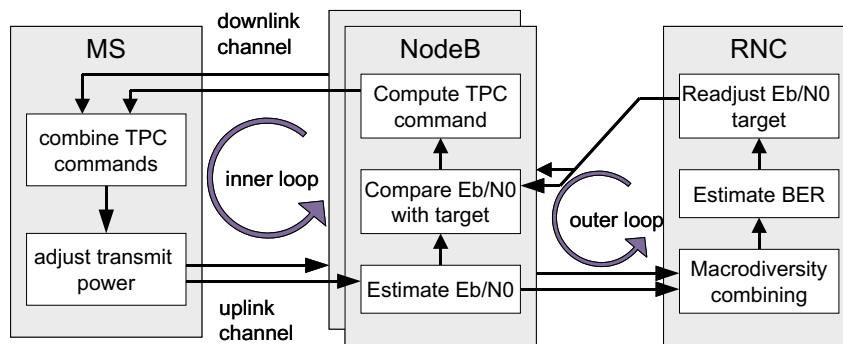
Figure 1. WCDMA uplink closed loop power control

The closed loop power control on the uplink consists of two interoperating loops [2,17], see Fig. 1. Within the *inner loop*, the NodeB continuously monitors the quality of the uplink in terms of the received E_b/N_0 level and compares it with the outer loop target. If the received value is too high, the MS causes too much interference to its environment and it is told to decrease its power by a fixed step size. On the other hand, if the received E_b/N_0 is too low, the link quality is not sufficient and a "power-up" command is sent to the mobile. Such an inner loop correction is performed for each power control group, 15 times per frame, resulting in a rate of 1500 updates per second. It should also be noted that an MS in soft handover will be communicating with the *radio network controller* (RNC) via all base stations in its active

set. In this case it will also receive several power control commands on the downlink. The MS will combine the received power control commands and will only increase its power if all base stations in the active set will demand an increase in transmit power.

After the transmission of a frame is complete, power control enters the *outer loop* [18]. Each frame is checked for errors at the RNC and the outer loop target value is updated based on the current *frame error rate* (FER). While the actual outer loop uses the received FER for updating its target value, we will consider a simplified case in which we evaluate the bit error rate instead. The reason for this approximation is that the relationship between E_b/N_0 and FER is not straightforward, as it requires an inclusion of the error rates at modulation, interleaving, and channel coding. Therefore, we will map the relationship between E_b/N_0 and BER based on the modulation scheme. Fig. 2 presents the mean E_b/N_0 target results from simulations based on different BER limits.
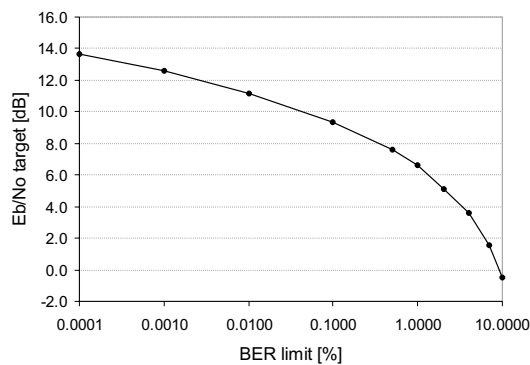
Figure 2. Measurement of E_b/N_0 target in relation to BER limit
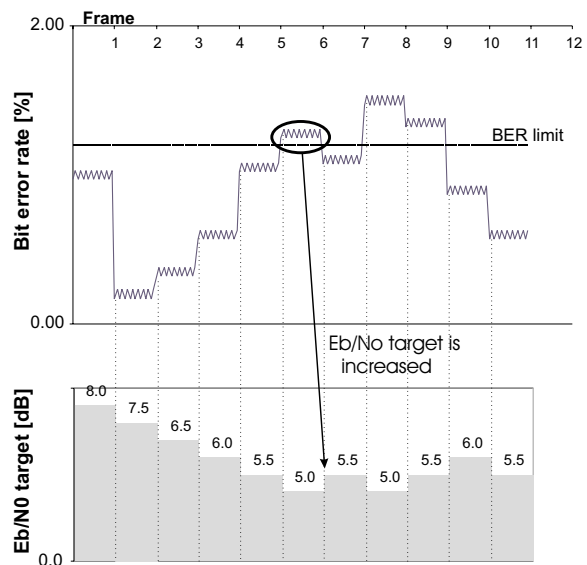
Figure 3. Correlation between the BER and E_b/N_0 target

For a better understanding of the effects of the bit error rate on the resulting E_b/N_0 target a simplified example is given in Fig. 3. The course of both BER and E_b/N_0 target is presented over a period of 11 frames. The bit error rate exhibits a typical behavior with variations from frame to frame. At the end of each frame the outer loop control adjusts the E_b/N_0 target depending on the current bit error rate. This means that if the BER exceeds the defined limit, the E_b/N_0 target has to be increased. Otherwise, this value will be reduced. So the course of the E_b/N_0 target is seen with regard to the bit error rate of each frame.

2.1. Approximation Method for Uplink Power Control

The major computational part of the simulation algorithm (cf. Fig. 1) consists of the inner loop calculation. The purpose of the simulation of power control groups lies in the stepwise adjustment of the mobile stations' transmit powers. Since the calculation time required for the simulation of a scenario often turns out as a limiting factor during detailed examinations, an inner loop algorithm is presented in this section that includes both, an approximation of the actual transmit power and a significant simplification of the extensive inner loop mechanism.

The basic idea behind this approximation algorithm is an estimation of the mean transmit power adjusted by the power control groups of an inner loop cycle. Since the inner loop mechanism updates the transmit power so that the current E_b/N_0 adapts to the E_b/N_0 target, a reverse calculation scheme is used as basis of the approximation (cf. Fig. 4).
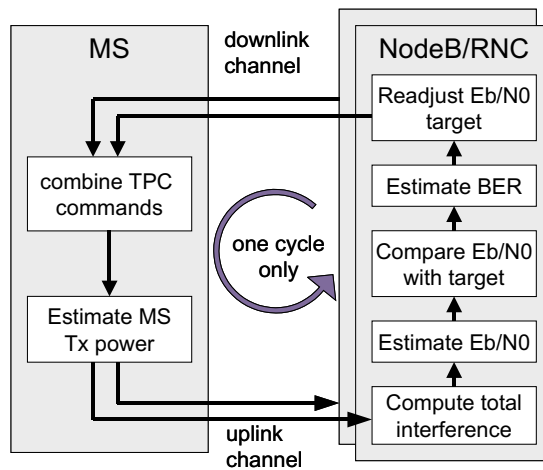
Figure 4. Approximated uplink power control loop

First of all the received interference of each mobile station has to be calculated. Using the E_b/N_0 target $\theta_i(t)$ and the interference $I_{o,i}(t)$ at frame t from all users without the considered user i, the received signal strength of the mobile station i can be written as

$$S_i(t) \quad = \quad \frac{R_i \, I_{o,i}(t) \, \theta_i(t)}{W}, \tag{1}$$

where R_i is the bit rate of the user and W the spreading bandwidth.

However, the actual other-user interference $I_{o,i}(t)$ is not known at this moment. Therefore, the value from the previous inner-loop cycle is used as an approximation instead.

$$I_{o,i}(t) \quad = \quad I_{\text{tot}}(t-1) - S_i(t-1), \tag{2}$$

where $I_{\text{tot}}(t-1)$ is the total received interference during frame $t-1$. Finally, the MS transmit power is the sum of $S_i(t)$ and $L_i(t)$, consisting of all losses from propagation, shadowing, etc.

$$T_i(t) \quad = \quad S_i(t) + L_i(t) \tag{3}$$

Because the complete inner loop cycle containing the simulation of the power control groups is now reduced to a single calculation step the required simulation time is reduced by a factor of 15 (corresponding to the 15 power control groups per frame in UMTS). This opens the way to simulating more detailed and complex scenarios as we will show in Section 4.

3. DERIVATION OF CELL LOADING AND NUMERICAL RESULTS

In this section we will give a description of the underlying simulation scenarios and the user and traffic distributions. For different reference scenarios, we will show the impacts of the user density in terms of the mean number of users per unit area size on the distribution of the interference received at a certain cell site. The interference for different traffic distributions leads to the derivation of the cell loading, which reduces the traffic description to a single value.

3.1. Scenario Description
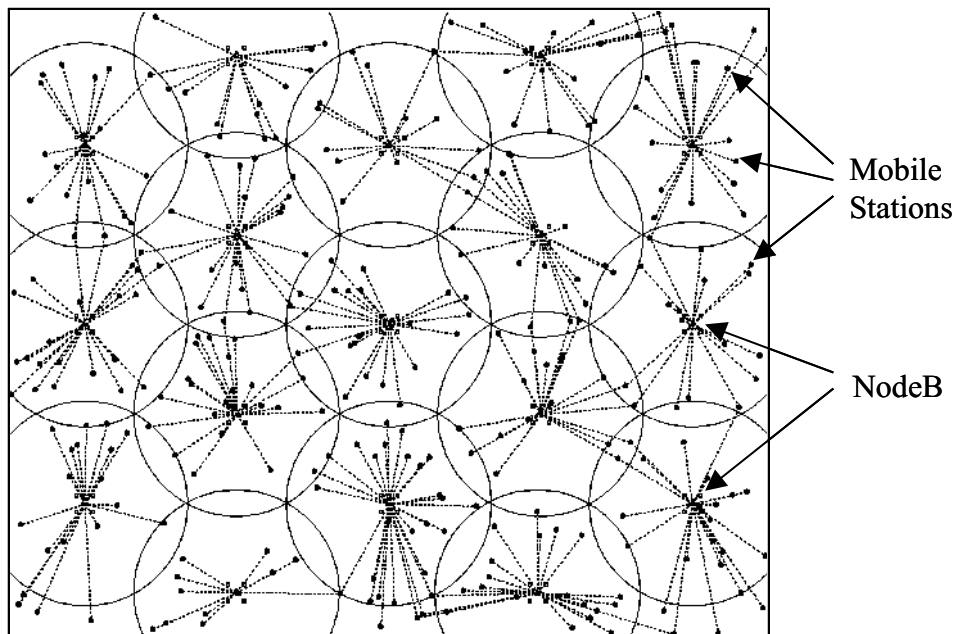
Figure 5. Cell layout used in simulations

Let us consider in the following a regular base station layout as depicted in Figure 5. Cell sizes are illustrated here with their pilot signal ranges, a parameter which is kept constant throughout the simulation. Within the considered area, users are randomly generated following a spatial homogeneous Poisson process [19]. In order to consider individual data rates, we selected for all cells the traffic mixes and the desired E_b/N_0 target level from Table 1, cf. [20], and a step size of 0.5 dB was chosen for the inner loop correction.

A fixed distance of 2 km between each base station was chosen. All simulation runs were performed over a duration of 15000 power control groups corresponding to a simulation time

	12.2 kbps	144 kbps	384 kbps
E_b/N_0 target	6 dB	3 dB	3 dB
mix1	100%	—	—
mix2	—	100%	—
mix3	—	—	100%
mix4	75%	20%	5%

Table 1
Traffic mixes and E_b/N_0 targets

of 10 seconds after a warm-up period of 5 seconds.

3.2. Evaluation of Inter-Cell and Intra-Cell Interference

The first value that we will investigate is the cumulative interference, distinguished in interference caused by users in the same cell due to the quasi-orthogonality of the codes (*intra-cell interference*) and the influence from users of the surrounding tiers of cells on our observed center cell (*inter-cell interference*). Both terms together constitute the term which we will denote as *total interference* I_{tot}.
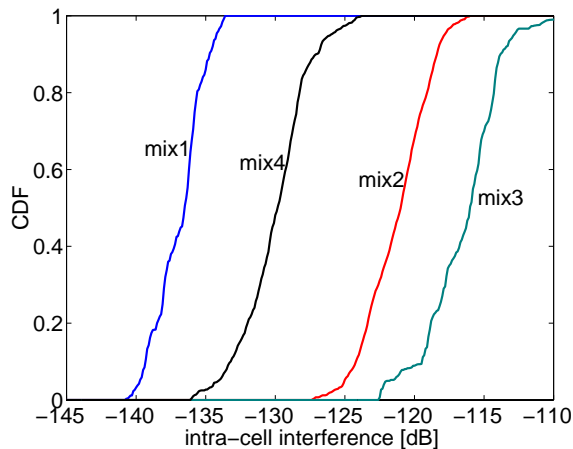
Figure 6. CDF of intra-cell interference for traffic mix 1-4
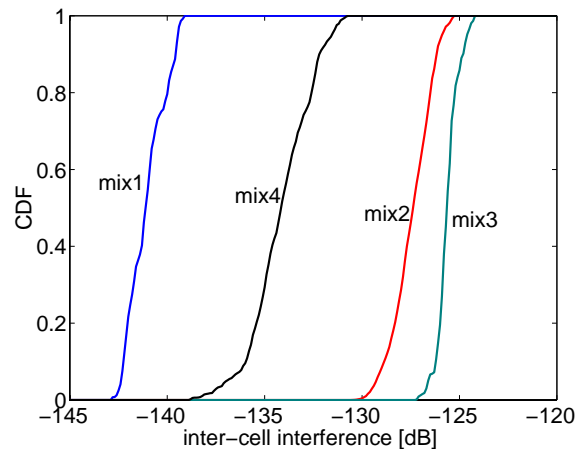
Figure 7. CDF of inter-cell interference for traffic mix 1-4

In Fig. 6 the cumulative probability distribution function (CDF) of the intra-cell interference is depicted for a fixed scenario with a mean traffic density of 4 users per km^2. Due to the higher spreading gain for 12.2 kbps users in mix1, the least interference is created here. The higher the data rates are, the higher is also the interference. Furthermore, it can be seen that using mix4, which is a combination of different data rates leads to a slightly larger variance. In Fig. 7 a similar observation can be made for the inter-cell interference. It can also be seen that the

inter-cell interference has a smaller mean and variance than the curves in Fig. 6. Again, the mix of several different data rates results in a higher variance.
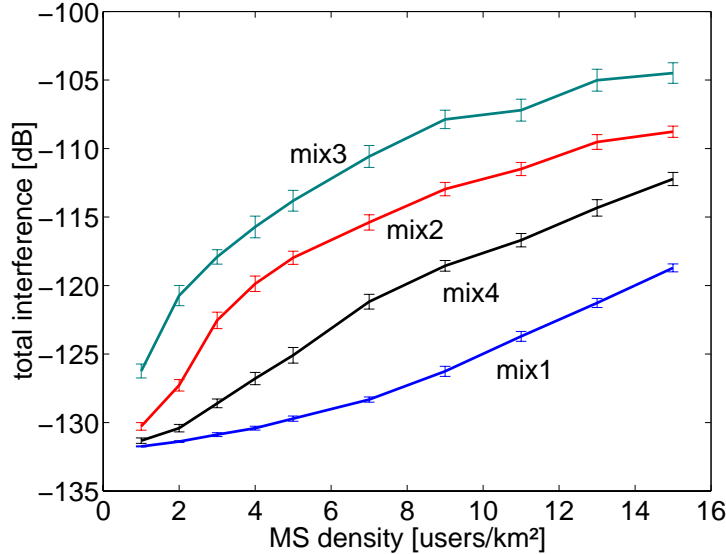
Figure 8. Mean total interference as function of MS density

The influence of the user density on the mean total interference is illustrated in Fig. 8. Depending on the traffic mix, the mean interference increases with the user density, for higher data rates the increase is more steep and saturates when the user density gets higher and the power control loops fail to achieve the target values. The outage rate will then increase as well. The error bars in Fig. 8 give the 95% confidence intervals obtained from 30 runs.

Fig. 9 shows the CDF of the total interference power for traffic mix4, where the full inner and outer loop simulation is compared with the inner loop approximation described in Section 2.1. It can be seen that for low interference the approximation matches the full loop quite well, however, for higher values the lack of the fine tuning in the inner loop leads to a slight overestimation of the transmit power, which results in a higher overall interference.

3.3. Definition of Cell Loading

In CDMA systems with only a single class of users, capacity can be easily described by the number of users served in the cell and the theoretical maximum limits can be computed as *pole capacity* [21] . However, third generation networks will provide many different classes of services, each with an individual data rate, activity behavior, and QoS requirement given by the maximum BER that is tolerable for this application. In order to evaluate the capacity of a UMTS cell we will examine the term *cell loading* ρ which we will define as

$$\rho = \frac{E[I_{\text{tot}}]}{E[I_{\text{tot}}] + N_0}. \tag{4}$$
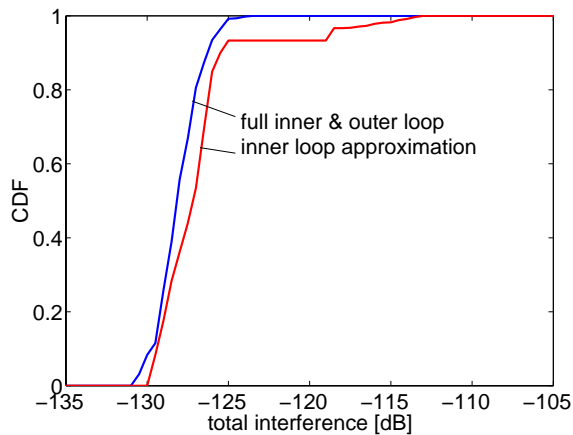
Figure 9. Comparison of inner loop approximation
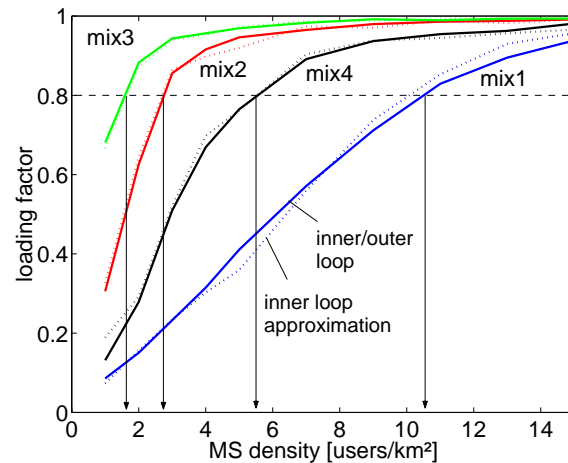
Figure 10. Cell loading as function of MS density

For an empty system without any user, the mean total interference $E[I_{\text{tot}}]$ will be zero and thus yields a load of zero. For increasing $E[I_{\text{tot}}]$, the influence of the N_0 term in the denominator will reduce and ρ approaches one. Note that often a different definition of the loading factor can be found, which considers the ratio of intra-cell interference to total interference [22]. This leads to the view of the load created in the considered cell, while we are more interested in a normalized interference term of the whole system.

In Fig. 10 the cell loading factor ρ is shown as a function of the MS density. It can be seen that ρ describes with one value a certain traffic situation, i.e., combinations of traffic mix and user density. Thus, a value of $\rho = 0.8$ could represent a load created for a user density of 10.5 for mix1 or a density of 5.5 when operating with traffic mix4.

3.4. Consideration of Outage Admission

So far, we considered that all MS would perform their power control loops regardless of the actually received E_b/N_0 of their connection. In the following we will examine the case when users are removed from the system, whenever their outage requirements are not fulfilled. We consider all users to be in *outage*, whenever their current E_b/N_0 falls below 0.5 dB under the E_b/N_0 target for a period of 1 second. Since we modeled all users to be active from the beginning of the simulation, we select the following method to remove users in outage. At first all users which exceed the E_b/N_0 target most are dropped and if after a recalculation of the interference situation other users are still in outage these would be dropped step by step as well.

In Fig. 11 and Fig. 12 the results for traffic mix4 from the previous sections are compared to the case when we remove users that are in outage. It can be seen that as long as we also consider users in outage for our interference calculation that would in reality drop their connection, we overestimate the total interference and cell loading. In fact the removal of outage users reduces the total interference up to 10 dB and the maximum load to about 85% instead of approaching 100%.
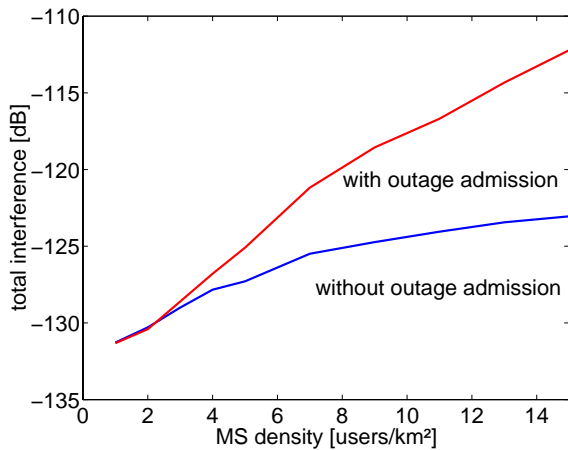
Figure 11. Mean total interference with outage admissions
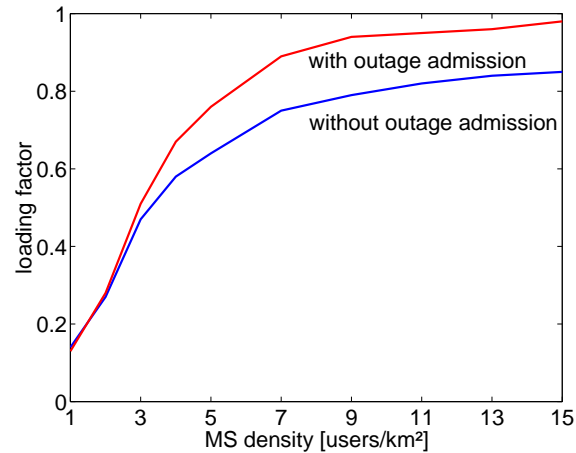
Figure 12. Influence of outage admissions on cell loading

4. EVALUATION OF COMPLEX SCENARIOS

The inner loop approximation now enables simulations of larger scenarios with complex characteristics. This section therefore demonstrates the measurement of cell parameters for a more realistic scenario. In view of network planning these results can be used to improve the base station arrangement in order to increase the coverage and enhance the quality of service of each user, see [3].

The scenario in this section uses data from the area around the city of Würzburg. A map of this area with an extension of 6.7 × 4.2 km is illustrated in Fig. 13. We assume that demands in teletraffic correspond to the density distribution of conventional traffic, i.e., more subscribers can be found on the main streets and in the city center than secondary streets. Only subscribers that are moving are used in this study. A fixed number of subscribers is distributed over the streets at the beginning of each simulation. These test users move during the simulation randomly on the road system – main streets are chosen preferably. Subscribers leaving the simulation area reenter the map again randomly at another incoming street. The number of test users, therefore, remains constant for the entire simulation time.

Contrary to the previous simplified studies, communication is now simulated on the basis of calls. This means, each test user begins and ends calls randomly. Therefore, we will use a slightly different method than in Section 3.4 to cope with outages. Since we have a session activity in this case, not all users will begin their connection at the same time instant. The criterion to drop outage users is given whenever the target BER can not be reached within 2 seconds.

The cell of interest is cell 5, where we will focus on the highlighted sector covering most parts of the city center with lots of streets with high density. In order to compare the results to a homogeneous case, we also select a Poisson process with the same average number of connections in a sector. However, unlike the Poisson case, in our Würzburg scenario there are
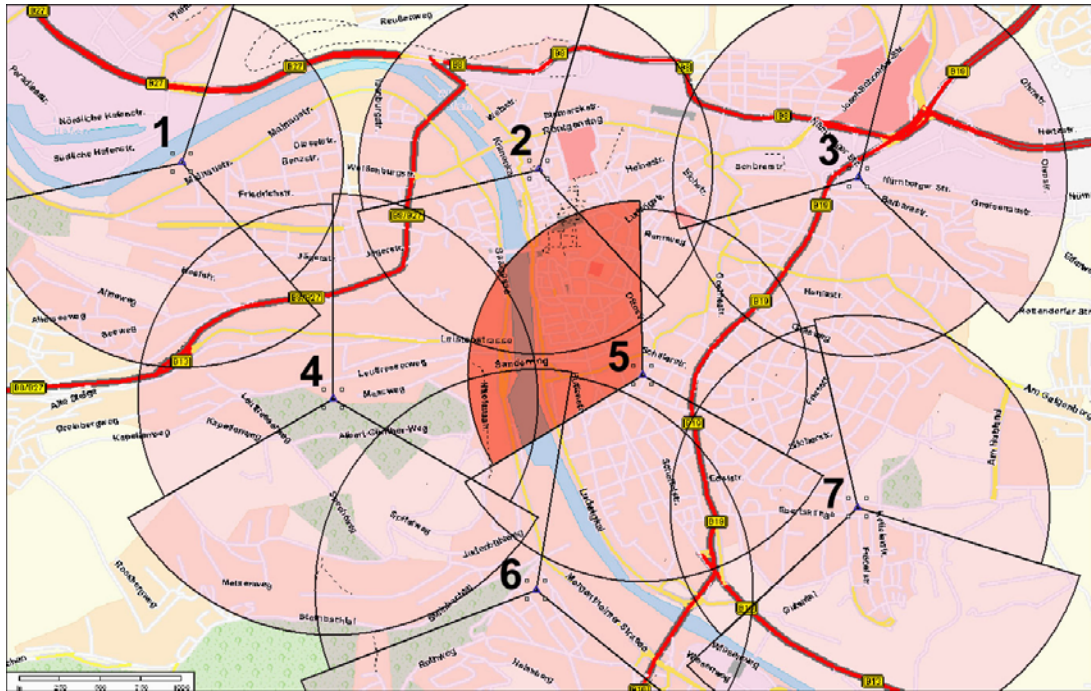
Figure 13. Realistic simulation scenario of the city of Würzburg

no stationary users.

In Fig. 14 the CDF of the total interference is given for traffic mix1 and mix4. It can be recognized that for mix4 there is a difference in mean of about 3 dB which shows that the homogeneous assumption leads to an underestimation of the total interference. For the more homogeneous traffic of mix1 (only voice users with 12.2 kbps) a good match between the Poisson model and the Würzburg model can be seen. Additionally, the inclusion of mobility in the Würzburg scenario causes the standard deviation of the total interference to increase by about 3 dB for mix4 and about 0.5 dB for mix1. Fig. 14 leads to the conclusion that it is possible to capture the basic effects of the traffic parameters on the interference in a homogeneous scenario, however, in order to perform an accurate prediction of the interference and load a detailed modeling of the location and movement of the users also plays an important role.

5. CONCLUSION

In this paper we presented a simulation model for evaluating the performance of a 3G wireless network operating with WCDMA. The capacity of such a system is greatly influenced by the performance of the closed loop power control. We therefore modeled the inner and outer loop uplink power control in great detail and derived empirical distributions of the intra-cell and inter-cell interference. It could be seen that changing the mix of traffic in the cells has an impact on the mean and variance of the received interference. Furthermore, we examined the loading factor as a descriptor of the traffic load which integrates the user density and the mix of
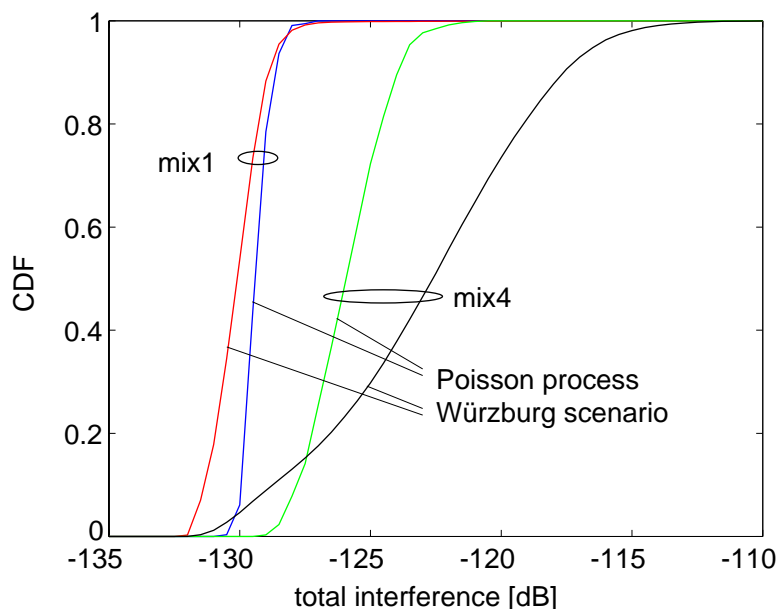
Figure 14. CDF of total interference for mix4

data rates into a single parameter.

We also showed that it is important to include the user reaction to outages since this results in calls to be dropped from not being able to maintain the E_b/N_0 target level and thus reduces the load in the cell. This indicates the need for an accurate model of the connection admission control mechanism implemented in the system.

The simulation time could be reduced by a factor of the inner loop updates per outer loop step when we only considered an approximated inner loop. It could be shown that the results were accurate enough for the evaluation of the cell loading and total interference. With this approximation of the power control loops, it is possible to investigate more complex scenarios with user mobility like the real world case which were considered in Section 4.

REFERENCES

1. F. Adachi, M. Sawahashi, H. Suda, Wideband DS-CDMA for next generation mobile communication systems, IEEE Communications Magazine .
2. H. Holma, A. Toskala, WCDMA for UMTS, John Wiley & Sons, Ltd., 2000.
3. U. Ehrenberger, K. Leibnitz, Impact of clustered traffic distributions in CDMA radio network planning, in: Proc. of ITC-16, Edinburgh, UK, 1999.
4. J. Zander, Transmitter power control for co-channel interference management in cellular radio systems, in: Proc. of 4th WINLAB Workshop, New Brunswick, NJ, 1993.
5. R. Pichna, Q. Wang, V. Bhargava, Non-ideal power control in DS-CDMA cellular, in: IEEE Pacific Rim Conference on Comm., Computers and Signal Processing, 1993, pp. 686–689.

6. R. D. Yates, A framework for uplink power control in cellular radio systems, IEEE Journal on Sel. Areas in Comm. 13 (7) (1995) 1341–1347.
7. K. Leibnitz, P. Tran-Gia, J. E. Miller, Analysis of the dynamics of CDMA reverse link power control, in: Proc. of IEEE Globecom 98, Sydney, Australia, 1998.
8. K. Leibnitz, Impacts of power control on outage probability in CDMA wireless systems, in: Proc. of the 5th Int. Conf. on Broadband Communications, Hong Kong, 1999, pp. 225–234.
9. S. Ariyavisitakul, L. F. Chang, Signal and interference statistics of a CDMA system with feedback power control, IEEE Trans. on Comm. 41 (11) (1993) 1626–1634.
10. R. D'Avella, D. Marizza, L. Moreno, Power control in CDMA systems: Performance evaluation and system design implications, San Diego, CA, 1994, pp. 73–77.
11. M. Jeong, D. D. Lee, D. H. Kim, Y. J. Chung, K. C. Whang, The performance of SIR-based power control in cellular CDMA system with mobility, in: The 2nd International Workshop on Multi-Dimensional Mobile Communications (MDMC96), 1996, pp. 695–699.
12. A. Chockalingam, P. Dietrich, L. B. Milstein, R. R. Rao, Performance of closed-loop power control in DS-CDMA cellular systems, IEEE Trans. on Veh. Tech. 47 (3) (1998) 774–789.
13. B. Hashem, N. Secord, Combining of power commands received from different base stations during soft handoff in cellular CDMA systems, in: Proc. of International Symposium on Personal, Indoor and Mobile Radio Communications PIMRC, Osaka, Japan, 1999.
14. H. Morikawa, T. Kajiya, T. Aoyama, A. T. Campbell, Distributed power control for various QoS in a CDMA wireless system, IEICE Trans. Fundamentals E80-A (12).
15. H. Suda, H. Kawai, F. Adachi, A fast transmit power control based on markov transition for DS-CDMA mobile radio, IEICE Trans. Commun. E82-B (8).
16. K. Sipilä, J. Laiho-Steffens, A. Wacker, M. Jäsberg, Modeling the impact of the fast power control on the WCDMA uplink, in: Proc. of VTC'99 Spring, Houston, TX, 1999.
17. 3GPP, Physical layer procedures (FDD), Report TR25.214, 3GPP, TSG RAN (2000).
18. A. Sampath, P. S. Kumar, J. M. Holtzman, On setting reverse link target SIR in a CDMA system, in: Proc. of the 47th IEEE Veh. Tech. Conf., Phoenix, AZ, 1997.
19. J. Kingman, Poisson Processes, Vol. 3 of Oxford Studies in Probability, Oxford University Press, New York, 1993.
20. 3GPP, RF system scenarios, Report TR25.942, 3GPP, TSG RAN WG4 (Sep. 2000).
21. V. V. Veeravalli, A. Sendonaris, The coverage-capacity tradeoff in cellular CDMA systems, IEEE Trans. on Veh. Tech. 48 (5).
22. T. Ojanperä, R. Prasad, Wideband CDMA for Third Generation Mobile Communications, Artech House, 1998.